Title
Longitudinal, multimodal functional imaging of microvascular response to photothermal therapy.

Journal
Optics Letters, 35(19)

ISSN
0146-9592

Authors
Bui, Albert K
Teves, Kathleen M
Indrawan, Elmer
et al.

Publication Date
2010-10-01

DOI
10.1364/ol.35.003216

Published in final edited form as:
Opt Lett. 2010 October 1; 35(19): 3216–3218.

Longitudinal, multimodal functional imaging of microvascular response to photothermal therapy

Albert K. Bui[1,2], **Kathleen M. Teves**[2,3], **Elmer Indrawan**[2,4], **Wangcun Jia**[2], and **Bernard Choi**[2,4,5,*]

[1]Jefferson Medical College, Thomas Jefferson University, Philadelphia, Pennsylvania 19107, USA

[2]Beckman Laser Institute and Medical Clinic, Department of Surgery, University of California, Irvine, California 92612, USA

[3]Department of Neurobiology, University of California, Irvine, California 92697, USA

[4]Department of Biomedical Engineering, University of California, Irvine, California 92697, USA

[5]Edwards Lifesciences Center for Advanced Cardiovascular Technology, University of California, Irvine, California 92697, USA

Abstract

Although studies have shown that photothermal therapy can coagulate selectively abnormal vasculature, the ability of this method to achieve consistent, complete removal of the vasculature is questionable. We present the use of multimodal, wide-field functional imaging to study, in greater detail, the biological response to selective laser injury. Specifically, a single-platform instrument capable of coregistered fluorescence imaging and laser speckle imaging was utilized to monitor vascular endothelial growth factor gene expression and blood flow, respectively, in a transgenic rodent model. Collectively, the longitudinal, *in vivo* data collected with our instrument suggest that the biological response to selective laser injury involves early-stage redistribution of blood flow, followed by increased vascular endothelial growth factor promoter activity to stimulate pro-angiogenic events.

Biological tissue requires a dense vascular system to supply nutrients and oxygen to tissue and remove toxic by-products produced by normal cellular processes. Various diseases lead to progressive alterations in microvascular architecture. For example, with port wine stain (PWS) birthmarks, abnormal neuronal signaling is implicated in development of capillary malformations in the skin [1]. The gold-standard treatment for these birthmarks has involved the use of pulsed lasers to photocoagulate selectively the abnormal vasculature [2].

Although studies have shown that pulsed-laser therapy can photocoagulate PWS vessels, the ability of this method to achieve consistent, complete removal of the birthmark is questionable [3,4]. We associate the limited efficacy to our incomplete understanding of the vascular repair response to selective laser-induced damage.

In this Letter, we present the use of multimodal, wide-field functional imaging (WiFI) to study, in greater detail, the biological response to selective laser injury. Specifically, a single-platform instrument capable of coregistered fluorescence imaging and laser speckle

*Corresponding author: choib@uci.edu.

imaging (LSI), was utilized to monitor vascular endothelial growth factor (VEGF) gene expression and blood flow, respectively.

To investigate the vascular repair process, a transgenic C3H mouse model [5] was used. To enable direct, chronic imaging of the microvasculature, a dorsal window chamber was surgically installed on each animal [5–9]. All animal-related procedures were approved by the Institutional Animal Care and Use Committee at University of California, Irvine.

Our animal model emits green fluorescent protein (GFP) under control of the VEGF promoter. Because VEGF plays a major role in angiogenesis [5,10,11], the presence of GFP emission indicates VEGF gene expression and, thus, is indicative of an angiogenic response. Concurrently, LSI was used to monitor changes in micro-vascular blood flow in response to selective laser injury.

Upon completion of window chamber installation, the animal was placed on a circulating-water heating pad positioned within a light-tight enclosure designed to mitigate stray light contamination of the fluorescence and speckle signals (Fig. 1). The window chamber was attached to a custom aluminum mount to image directly the subdermal microvasculature that is exposed after surgery. A mixture of isoflurane gas (2%–5%) and oxygen was used as inhalation anesthesia during each imaging session. A 12 bit, thermoelectrically cooled CCD camera was mounted above the enclosure. A variable-magnification (0:7× to 4×) lens was used to image the window chamber onto the CCD sensor. An ~30 mm diameter observation port was created in one wall of the enclosure to enable imaging of the *in vivo* preparation.

Images were collected with three imaging modes: (1) architectural imaging—the window chamber was transilluminated with broadband light delivered from a broadband tungsten–halogen lamp, (2) LSI—the window chamber was transilluminated with coherent 633 nm He–Ne laser light, and (3) fluorescence imaging—the window chamber was epiilluminated with 488 nm light. For fluorescence imaging, an external bandpass filter (center wavelength of 530 nm) was used to collect selectively the GFP fluorescence emission.

Previous studies [7,12–15] have demonstrated the ability of LSI to quantify blood-flow dynamics in the dorsal window chamber. In these studies, short exposure times (e.g., 10 ms) were used. However, the use of short exposure times hinders the ability of LSI to enable visualization of blood flow in capillaries and small arterioles and venules. To enable functional vascular density mapping using LSI principles, we instead employed long exposures times (e.g., >1000 ms) to enable visualization of vessel perfusion in both large and small microvasculature, albeit at a loss of quantifiable blood flow (Fig. 2). Long-exposure LSI enables functional vascular density mapping without the need for exogenous intravascular contrast agents, such as fluorescein isothiocyanate dextran or Texas Red.

We used our WiFI instrument to achieve coregistered fluorescence and long-exposure (5000 ms) LSI images during longitudinal experiments in which the window chamber vasculature was irradiated with pulsed laser light. A frequency-doubled Nd:YAG laser (DualisVP, Fotona Laser, Ljublijana, Slovenia) was used to irradiate a specific arteriole–venule pair (diameters of ~100 μm) using an ~2 mm spot size. Based on previous published data [7,15], laser parameters (3 pulses, 1 ms pulse duration, 20 Hz repetition rate, 5:0 J/cm^2) that reliably achieve acute vessel photocoagulation, were selected. Fluorescence and LSI images were collected prior to and immediately following laser irradiation (i.e., Day 0). Raw speckle data were converted to maps of relative blood flow using a simplified speckle imaging equation [16]. Follow-up images were collected at Days 1, 3, and 7 postirradiation, at magnifications of 1× and 4×.

Prior to laser irradiation, LSI images showed obvious blood flow at the site of interest (Fig. 3). After irradiation, an immediate disruption of flow was observed, signifying that acute photocoagulation was achieved. With subsequent images taken on Days 1, 3, and 7, we visualized a progressive increase in the number of perfused vessels surrounding the injured site. Interestingly, Day 3 showed increased blood flow in the irradiated vessel, with flow stoppage observed by Day 7. We hypothesize that these events represented an initial hyperemic response in an injured, constricted vessel, which ultimately failed to remain patent. As a result, recruitment of macrophages during the ensuing wound healing response may have initiated breakdown of the injured vessel, hence resulting in an absence of blood flow at Day 7.

We concurrently observed GFP fluorescence emission within and surrounding the irradiated site, indicative of increased VEGF gene expression and, hence, angiogenesis-stimulating activity (Fig. 3). Our preliminary data ($n = 3$) have consistently shown peak GFP emission at Day 7. Since this GFP signal comes from fibroblasts, which are cells involved in extracellular matrix secretion and wound healing, the strong fluorescent signal seen on Day 7 (i.e., after blood flow stopped in the laser irradiated vessel), suggests that the resulting hypoxic environment promoted secretion of growth factors, like VEGF, to remodel the microvasculature.

Since angiogenesis is a process that develops over days to weeks following injury, the immediate (i.e., Day 0, postlaser irradiation) increase in the number of perfused vessels surrounding the irradiated site is most likely due to redistribution of blood flow to collateral vessels, as observed previously [7]. Therefore, in addition to the proangiogenic activity suggested by the progressive increase in GFP emission, increased perfusion and dilation of existing vessels appear to play a key part in the microvascular repair response after selective laser injury.

Collectively, the longitudinal *in vivo* data collected with our WiFI instrument suggest that the biological response to selective laser injury involves early-stage redistribution of blood flow, followed by increased VEGF promoter activity to stimulate proangiogenic events. Additional experiments are planned to study the (1) effects of severity of microvascular injury (i.e., high irradiance versus low irradiance), (2) type of microvascular injury (i.e., photothermal versus photochemical), and (3) modulation of the angiogenic response using antiangiogenic agents [15,17]. Furthermore, with integration of other camera-based optical modalities, such as hemoglobin oxygen saturation imaging [9,18], we plan to obtain a detailed picture of the overall biological response to selective optical injury modalities.

Acknowledgments

We thank Rakesh Jain and Dai Fukumura, Steele Laboratories, Massachussetts General Hospital, for their generous donation of the transgenic animal model used in the research. Funding for this research was provided in part by the Arnold and Mabel Beckman Foundation, the National Institutes of Health (NIH) (EB009571), and the National Institutes of Health Laser Microbeam and Medical Program (LAMMP, a P41 Technology Research Resource).

References

1. Mulliken, JB.; Young, AE. Vascular Birthmarks: Hemangiomas and Malformations. W. B. Saunders; 1988.
2. Anderson RR, Parrish JA. Lasers Surg. Med. 1981; 1:263. [PubMed: 7341895]
3. Le KVT, Shahidullah H, Frieden IJ. Dermatol. Surg. 1999; 25:127. [PubMed: 10037519]
4. Jasim ZF, Handley JM. J. Am. Acad. Dermatol. 2007; 57:677. [PubMed: 17658196]
5. Fukumura D, Xavier R, Sugiura T, Chen Y, Park EC, Lu NF, Selig M, Nielsen G, Taksir T, Jain RK, Seed B. Cell. 1998; 94:715. [PubMed: 9753319]

6. Papenfuss HD, Gross JF, Intaglietta M, Treese FA. Microvasc. Res. 1979; 18:311. [PubMed: 537508]
7. Choi B, Jia WC, Channual J, Kelly KM, Lotfi J. J. Invest. Dermatol. 2008; 128:485. [PubMed: 17657245]
8. Barton JK, Vargas G, Pfefer TJ, Welch AJ. Photochem. Photobiol. 1999; 70:916. [PubMed: 10628303]
9. Sorg BS, Moeller BJ, Donovan O, Cao YT, Dewhirst MW. J. Biomed. Opt. 2005; 10:044004.
10. Ferrara N. J. Mol. Med. 1999; 77:527. [PubMed: 10494799]
11. Veikkola T, Alitalo K. Sem. Can. Biol. 1999; 9:211.
12. Choi B, Kang NM, Nelson JS. Microvasc. Res. 2004; 68:143. [PubMed: 15313124]
13. Channual J, Choi B, Pattanachinda D, Lotfi J, Kelly KM. Lasers Surg. Med. 2008; 40:644. [PubMed: 18951421]
14. Jia WC, Choi B, Franco W, Lotfi J, Majaron B, Aguilar G, Nelson JS. Lasers Surg. Med. 2007; 39:494. [PubMed: 17659588]
15. Jia WC, Sun V, Tran N, Choi B, Liu SW, Mihm MCJ, Phung TL, Nelson JS. Lasers Surg. Med. 2010; 42:105. [PubMed: 20166161]
16. Ramirez-San-Juan JC, Ramos-Garcia R, Guizar-Iturbide I, Martinez-Niconoff G, Choi B. Opt. Express. 2008; 16:3197. [PubMed: 18542407]
17. Phung TL, Oble DA, Jia W, Benjamin LE, Mihm MC, Nelson JS. Lasers Surg. Med. 2008; 40:1. [PubMed: 18220264]
18. Dunn AK, Devor A, Bolay H, Andermann ML, Moskowitz MA, Dale AM, Boas DA. Opt. Lett. 2003; 28:28. [PubMed: 12656525]

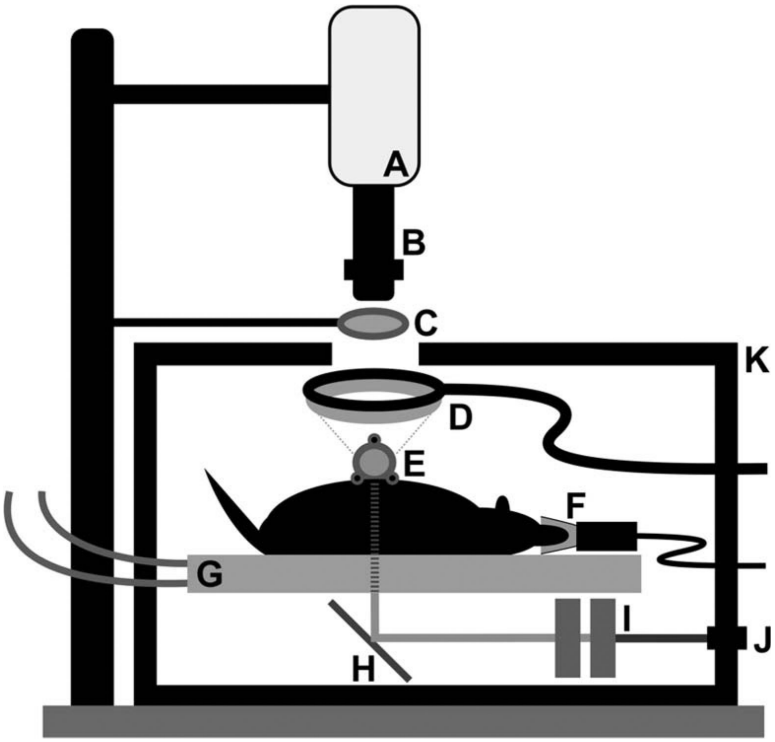

Fig. 1.

Schematic of experimental setup used to monitor VEGF promoter activity and blood flow in the dorsal window chamber microvasculature in response to selective laser injury. A, CCD camera; B, zoom lens; C, 532 nm emission filter; D, ring-light illuminator (488 nm excitation); E, window chamber; F, anesthesia nose cone; G, heating bed (to water heater/circulator); H, mirror; I, dual polarizers for attenuation; J, modular light port (633 nm He–Ne and white halogen); K, light-tight enclosure.

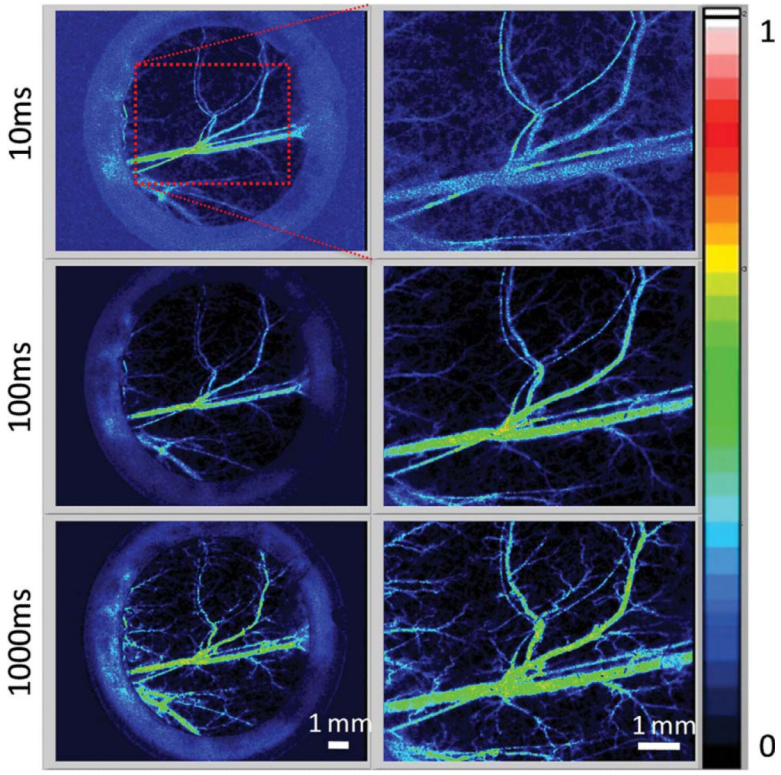

Fig. 2.

(Color online) Representative normalized blood-flow maps derived from raw speckle images, using LSI-based analysis with a simplified speckle imaging equation. Blood-flow maps are shown at 1× (left) and 2× (right) optical magnification taken at exposure times of 10, 100, and 1000 ms. Note the increase in discernible vasculature in the blood-flow maps taken with longer exposure times.

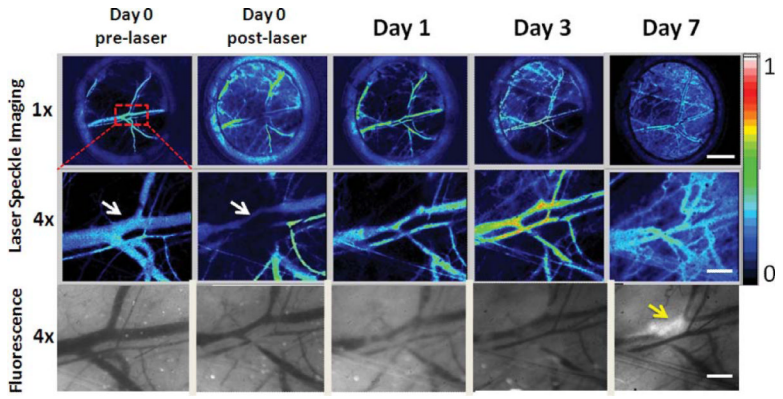

Fig. 3.

(Color online) Representative mouse dorsal window chamber imaged on Days 0 (pre-laser and post-laser irradiation), 1, 3, and 7, at 1× (top row) and 4× (middle and bottom rows) optical magnifications, to observe the vascular repair response to selective laser injury. Normalized blood-flow maps were collected using a 5000 ms exposure time. Note the presence of blood flow before laser irradiation (compared to the disruption of blood flow following laser irradiation (white arrows in middle row). Based on subsequent image sets taken on Days 1, 3, and 7, we observed a progressive increase in the number of perfused vessels surrounding the injured site. Concurrently, we observed an increase in 530 nm fluorescence emission (bottom row) immediately surrounding the postinjury site, indicating GFP/VEGF activity, with a peak signal on Day 7 (yellow arrow at bottom right). Scale bars: 1× images (2 mm), 4× images (1 mm).